



# A little mica goes a long way: Impact of phyllosilicates on quartz deformation fabrics in naturally deformed rocks

Raphaël Gottardi<sup>1,2,\*</sup>, Gabriele Casale<sup>3</sup>, John Economou<sup>2</sup>, and Kristen Morris<sup>2</sup>

<sup>1</sup>Department of Geosciences, Auburn University, Auburn, Alabama 36849, USA

<sup>2</sup>School of Geosciences, University of Louisiana at Lafayette, Lafayette, Louisiana 70504, USA

<sup>3</sup>Department of Geological and Environmental Sciences, Appalachian State University, Boone, North Carolina 28608, USA

## ABSTRACT

Quartz deformation fabrics reflect stress and strain conditions in mylonites, and their interpretation has become a mainstay of kinematic and structural analysis. Quantification of grain size and shape and interpretation of textures reflecting deformation mechanisms can provide estimates of flow stress, strain rate, kinematic vorticity, and deformation temperatures. Empirical calibration and determination of quartz flow laws is based on laboratory experiments of pure samples; however, pure quartzite mylonites are relatively uncommon. In particular, phyllosilicates may localize and partition strain that can inhibit or enhance different deformation mechanisms. Experimental results demonstrate that even minor phyllosilicate content (<15 vol%) can dramatically alter the strain behavior of quartz; however, few field studies have demonstrated these effects in a natural setting.

To investigate the role of phyllosilicates on quartz strain fabrics, we quantify phyllosilicate content and distribution in quartzite mylonites from the Miocene Raft River detachment shear zone (NW Utah, USA). We use microstructural analysis and electron backscatter diffraction to quantify quartz deformation fabrics and muscovite spatial distribution, and X-ray computed tomography to quantify muscovite content in samples with varying amounts of muscovite collected across the detachment shear zone. Phyllosilicate content has a direct control on quartz deformation mechanisms, and application of piezometers and flow laws based on quartz deformation fabrics yield strain rates and flow stresses that vary by up to two orders of magnitude across our samples. These findings have important implications for the application of flow laws in quartzite mylonites and strain localization mechanisms in mid-crustal shear zones.

## INTRODUCTION

Quartz mylonites commonly contain secondary phases, such as phyllosilicates (e.g., Taylor and McLennan, 1985), which may play an important role in the dynamic recrystallization of quartz and other minerals (e.g., Song and Ree, 2007; Herwegen et al., 2011; Hunter et al., 2016; Wehren et al., 2017). Depending on the quantity and arrangement of phyllosilicates, quartz may change deformation processes (dislocation to diffusion creep), thereby affecting the rheology of the crust (e.g., Tullis and Yund, 1991). During the development of S-C fabrics associated with mylonitization, phyllosilicates form interconnected networks, causing a change in rheo-

logical properties in which the weak phase—phyllosilicates—accommodates strain, resulting in a weaker aggregate (e.g., Holyoke and Tullis, 2006). In addition, phyllosilicates inhibit dynamic recrystallization by grain boundary migration, preventing grain growth and encouraging other mechanisms such as dissolution creep, dislocation glide in phyllosilicates, and grain boundary sliding in quartz (e.g., Olgaard, 1990; Song and Ree, 2007; Hunter et al., 2016; Wehren et al., 2017). Inhibition of grain boundary migration leads to reduced dynamic grain growth, resulting in diminished grain size, which may cause the dominant deformation mechanism of the main phase to switch from grain-size-insensitive dislocation creep to grain-size-sensitive diffusion creep (e.g., Etheridge and Wilkie, 1979; Olgaard, 1990; De Bresser et al., 1998, 2001; Fukuda et al., 2018; Richter et al., 2018).

Because of this critical dependency of rheology on grain size, it is important to understand how weaker secondary phases such as phyllosilicates can affect grain size and thus, in turn, rheology.

The role of phyllosilicate in strain localization has been observed in experimental work (Tullis and Wenk, 1994) and proposed theoretically (Johnson et al., 2004; Gerbi et al. 2010; Montési, 2013; Rast and Ruh, 2021), but only a few studies have explored this in naturally deformed rocks (e.g., Kronenberg, 1981; Song and Ree, 2007; Herwegen et al., 2011; Wehren et al., 2017). Results from lab experiments conducted on quartz aggregates containing various amounts of muscovite indicate that when quartz deforms by dislocation creep, addition of as little as 10% muscovite causes a mechanical transition from a strong phase that forms a load-bearing framework to an aggregate with an interconnected weak phase, allowing strain partitioning into the weak muscovite network, thereby reducing the composite strength of the aggregate (e.g., Tokle et al., 2023).

This paper investigates the role of muscovite in quartz deformation. We focus on the Miocene Raft River detachment shear zone (RRDSZ) associated with the Raft River metamorphic core complex, NW Utah, USA (e.g., Compton, 1980). Quartz microstructural and electron backscatter diffraction (EBSD; e.g., Prior et al., 1999) analyses are combined with X-ray computed tomography (XRCT; e.g., Mees et al., 2003) to quantify muscovite content and its impact on quartz recrystallization mechanisms. Our results suggest that quartz recrystallized grain size (RxGS) varies significantly not only between different samples but also within each sample depending on the presence or absence of muscovite. These findings have important implications for the application of RxGS piezometers and dislocation creep flow law used to constrain the mechanical evolution of detachment shear zones.

Raphaël Gottardi  <https://orcid.org/0000-0002-6774-1343>  
\*gottardi@auburn.edu

CITATION: Gottardi, R., et al., 2024, A little mica goes a long way: Impact of phyllosilicates on quartz deformation fabrics in naturally deformed rocks: *Geology*, v. XX, p. , <https://doi.org/10.1130/G52053.1>

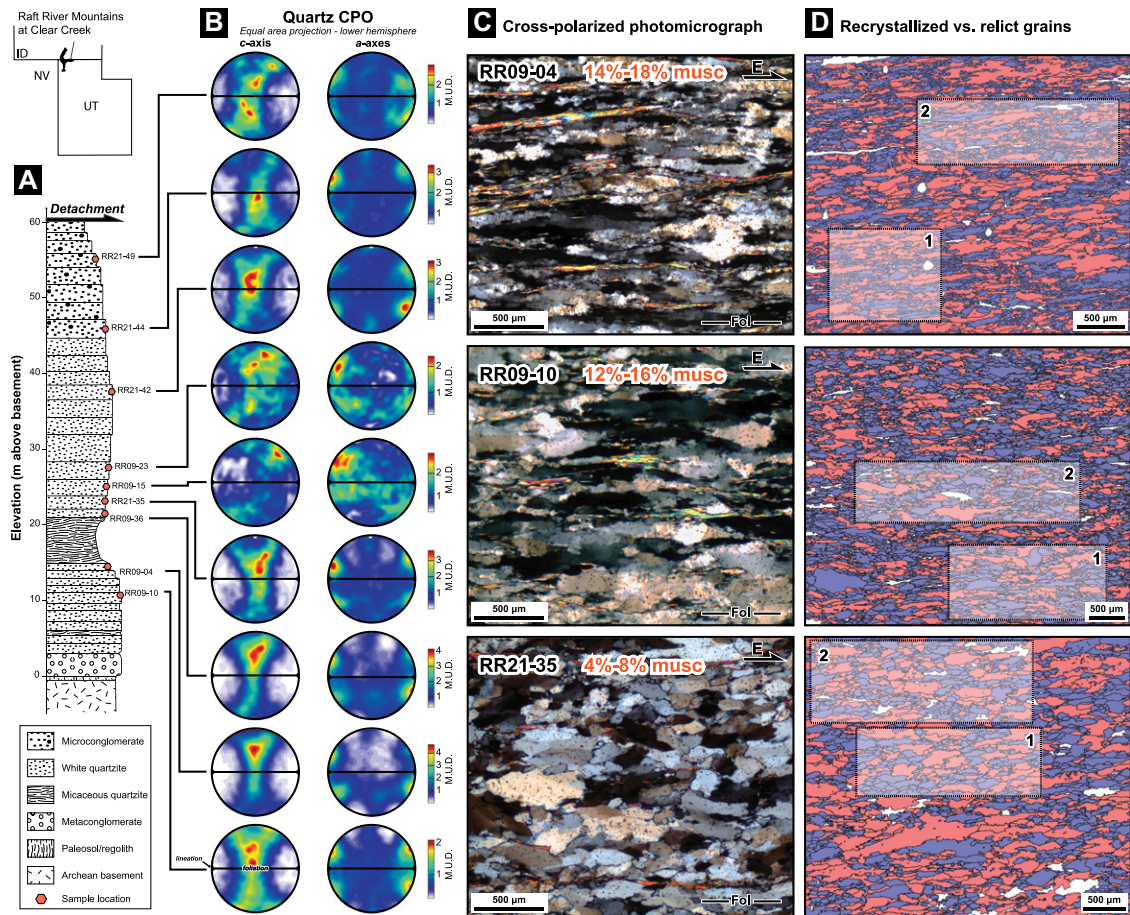


**Figure 1.** (A) Synthetic vertical profile of the Raft River detachment zone. (B) Electron backscatter diffraction (EBSD) pole figures of quartz *c*-axis and *a*-axes oriented like the thin sections shown in C. CPO—crystallographic preferred orientation; M.U.D.—multiples of uniform distribution. (C) Representative microstructures of the samples (cross-polarized thin section photos taken with polarizer oriented at  $\sim 45^\circ$  to foliation to maximize muscovite illumination). musc—muscovite; Fol—foliation. (D) EBSD maps showing recrystallized (blue) and relict (red) quartz grains and two subset areas: one consisting of pure quartz (zone 1) and one containing muscovite (zone 2).

## THE RAFT RIVER DETACHMENT SHEAR ZONE

The Raft River Mountains form the eastern limb of the larger Albion–Raft River–Grouse Creek metamorphic core complex in NW Utah (Fig. S1 in the Supplemental Material<sup>1</sup>; e.g., Compton, 1980). Exhumation of the RRDSZ initiated ca. 25–20 Ma and shows muscovite  $^{40}\text{Ar}/^{39}\text{Ar}$  ages as young as 15 Ma (Wells et al., 2000). The RRDSZ is best exposed along Clear Creek Canyon, incised along the transport direction, providing vertical exposures of continuous sections of mylonitic rocks (Fig. S1). The RRDSZ is localized in the  $\sim 100$ -m-thick Proterozoic Elba Quartzite (Compton, 1980). The mylonitic fabric is constant throughout the RRDSZ, characterized by sub-horizontal foliation, defined by flattened and elongated muscovite grains, and eastward stretching lineation (Compton, 1980). Quartz microstructures and stable isotope geothermometry suggest that Miocene mylonitization occurred under greenschist-facies conditions (345–485 °C; Gottardi et al., 2011).

## ANALYTICAL METHODS

Samples were collected along a vertical transect across the RRDSZ at Clear Creek Canyon, which contains a muscovite-rich horizon located  $\sim 15$ –22 m above the basement (Fig. 1A). The base of this horizon is characterized by a transition from cliff-forming Elba Quartzite to a zone where muscovite makes up 80%–100% of the rock. Microstructural analysis was conducted on thin sections oriented perpendicular to foliation and parallel to lineation. XRCT and EBSD analyses were conducted on  $\sim 5 \times 5 \times 5$  mm cubes cut from the thin section billets with the same orientation. Muscovite content was measured by XRCT at the University of Texas at Austin (USA) High Resolution XRCT Facility (see File S1 in the Supplemental Material). Quartz crystallographic preferred orientation was investigated by EBSD at Appalachian State University (Boone, North Carolina, USA) on the cubes imaged by XRCT (see File S1).

For each sample, the average RxGS (root mean square of the mean diameter) of the samples was estimated for (1) the entire sample surface, (2) a smaller muscovite-free area, and (3) a muscovite-rich area on each sample surface (Fig. 1; Table S1 [see footnote 1]). Differential stress was estimated based on the quartz RxGS piezometer of Cross et al. (2017). Strain rate was calculated using the quartzite dislocation creep flow law of Hirth et al.

(2001), with a stress exponent  $n$  of 4, an activation energy  $Q$  of 135 kJ/mol, and a temperature of 400 °C (Gottardi et al., 2011).

## RESULTS

The quartzite is characterized by two quartz grain populations: coarse elongate ( $> 500$   $\mu\text{m}$  long) “relict” grains and finer recrystallized grains (20–100  $\mu\text{m}$ ) (Fig. 2). The relict grains define the macroscopic fabric and exhibit undulose extinction and deformation lamellae (Fig. 2). Dynamic recrystallization textures reflect dominantly sub-grain rotation as described by Hirth and Tullis (1992) and consistent with previous observations of the RRDSZ (e.g., Gottardi and Teyssier, 2013). Petrographic observations and XRCT results demonstrate that the amount of muscovite varies among the samples, ranging from 4–8 vol% to 14–18 vol% (Fig. 3).

Quartz *c*-axes show Type I cross girdles indicative of basal, prism, and rhomb  $<\alpha>$  slip (Fig. 1). The structurally lowest three samples display a narrow girdle with a strong rhomb  $<\alpha>$  maxima and a slight dextral asymmetry indicative of top-to-the-east sense of shear.

The average RxGSs across all samples range from 20.6 to 60.5  $\mu\text{m}$ . We observe a negative correlation between grain size and muscovite content where the smallest RxGS is associated with the samples containing the most muscovite and vice

<sup>1</sup>Supplemental Material. Figure S1: Simplified geological map and cross section of the Raft River Mountains. Table S1: Quartz textural results from electron backscatter diffraction analysis. File S1: Analytical procedure. Please visit <https://doi.org/10.1130/GEOLOGICALSOCIETY.ORG/2554414> to access the supplemental material; contact [editing@geosociety.org](mailto:editing@geosociety.org) with any questions.



**Figure 2.** (A–D) Cross-polarized thin section photomicrographs of representative microstructures of the Raft River detachment shear zone quartzite mylonite. Relict and recrystallized grains are shown by black arrows. Yellow arrows indicate grain boundary pinning by muscovite. (E–G) Relict grains show undulose extinction (ue) and contain deformation lamellae (dl). Thin sections are cut perpendicular to foliation (Fol) and parallel to lineation; photos were taken with polarizer oriented at 45° to foliation to maximize muscovite illumination.

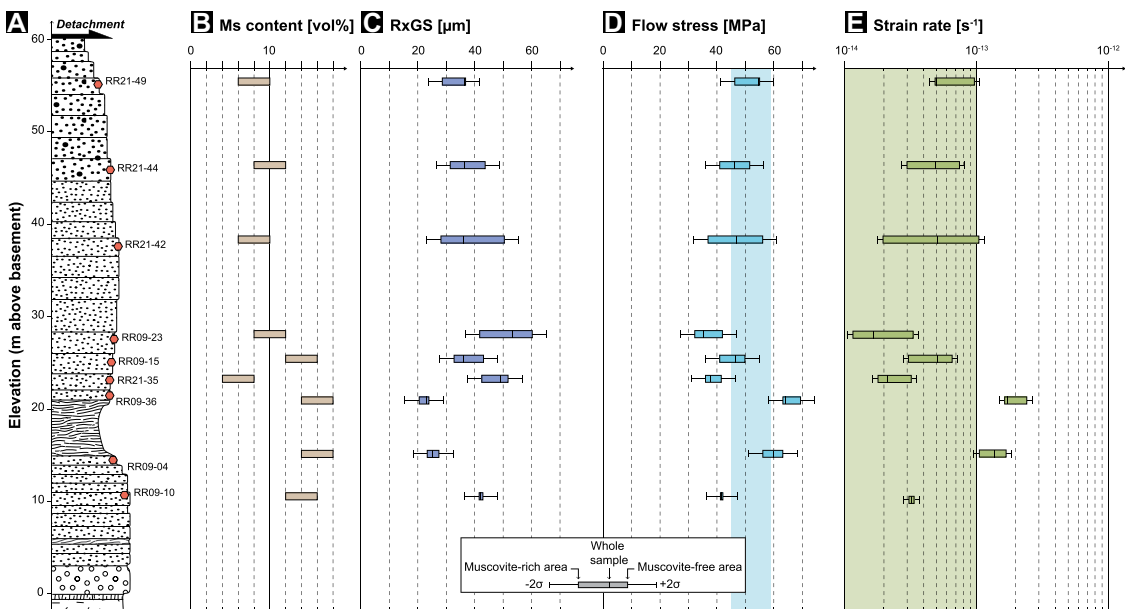


**Figure 3.** (A) Synthetic vertical profile of the Raft River detachment shear zone. See Figure 1A for symbol explanations. (B) Muscovite (Ms) content obtained from X-ray computed tomography. (C) Root mean square of mean diameter of recrystallized quartz grain (RxGS) obtained by electron back-scatter diffraction analysis. (D) Flow stress estimates using the Cross et al. (2017) piezometer. (E) Strain rate estimates based on the Hirth et al. (2001) quartzite flow law. Semi-transparent blue and green boxes indicate independent flow stress and strain rate estimates, respectively, for the Raft River detachment shear zone (see text for discussion).

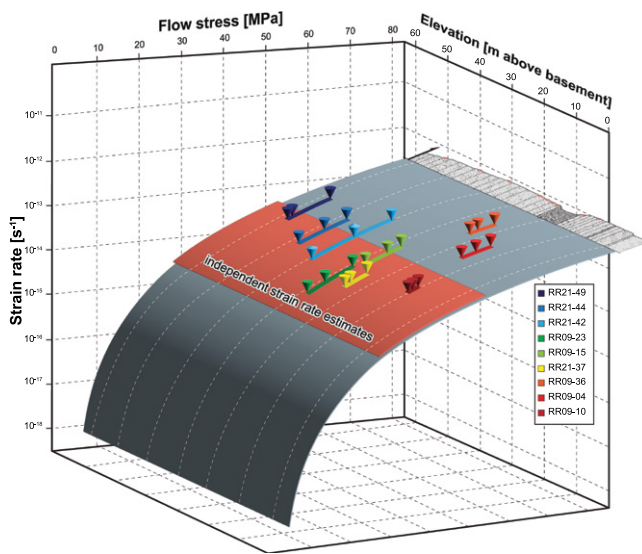


**Figure 4.** Flow stress versus strain rate versus elevation of the analyzed samples. Grey shaded surface represents strain rate calculated using the Hirth et al. (2001) quartzite flow law at 400 °C. Red shaded area refers to independent strain rate estimates of Gottardi and Teyssier (2013).

versa (Fig. 3). Similarly, grain size analysis of muscovite-free and muscovite-rich areas reveals that the RxGS is systematically smaller in the muscovite-rich area than in the muscovite-free area or than the average grain size of all samples except for RR09-10. The grain size spread between muscovite-free and muscovite-rich areas ranges from 0.9 to 22.4  $\mu\text{m}$  across our sample suite (2%–62% variation with respect to bulk grain size) (Fig. 3; Table S1). Based on our RxGS, we use the Cross et al. (2017) quartz RxGS piezometer to estimate differential stress, which ranges from 32.3 to 69.4 MPa, and estimate the strain rate to be between  $1.1 \times 10^{-14}$  to  $2.4 \times 10^{-13} \text{ s}^{-1}$  using the Hirth et al. (2001) quartzite dislocation creep flow law (Fig. 3; Table S1).

## DISCUSSION

Our findings are consistent with lab results that suggest even minor phyllosilicate content (<10%) exerts significant control on quartz deformation (e.g., Tokle et al., 2023). Samples sharing similar microstructures and dislocation creep deformation processes collected within a 50-m vertical transect show an inverse relationship between RxGS and muscovite content (Fig. 3), ranging from 53.3  $\mu\text{m}$  to 23.1  $\mu\text{m}$  correlating to ~6 vol% to ~16 vol% muscovite, respectively. Additionally, RxGS varies within each sample, to as large as 22.4  $\mu\text{m}$  (Table S1; Fig. 3). The observed correlation between muscovite content and quartz deformation textures has substantial implications for the application of piezometry and strain rate estimates, which are ultimately based on quartz RxGS. The observed RxGS variability translates to a ~32–70 MPa range in flow stress and a range in strain rates of more than one order magnitude (~ $1.1 \times 10^{-14}$  to  $2.4 \times 10^{-13} \text{ s}^{-1}$ ) across all samples (Table S1; Fig. 3). Intra-sample grain size variation correlated to muscovite content results in a difference of flow stress of ~10 MPa and more than an order of magnitude in strain rate.

Microscale bands of contrasting grain sizes have been interpreted elsewhere to record progressive superposition of deformation fabrics and used to track the evolution of local deformation or metamorphic conditions (e.g., Behr and Platt, 2011). Textural variation within individual samples correlates to a strain rate difference of more than one order of magnitude (Fig. 3), which could similarly be interpreted as being due to superposed fabrics recording an evolving detachment shear zone. However, this interpretation requires extreme deformation temperature gradients and strain rate and/or flow stress localization, or reactivation of the detachment shear zone.

If we assume that differences in RxGS are due to temperature, then our observed RxGS range would translate to a difference in temperature of 75–100 °C across our samples. Detachment shear zones can show apparent large temperature ranges because high-strain zones can telescope rocks that have experienced broadly different thermal conditions (e.g., Law et al., 2011). However, there is no evidence of such structures that would juxtapose rocks with different thermal histories in the RRDSZ. Quartz microstructures and dominant deformation mechanism are consistent across all our samples and the broader RRDSZ (Fig. 1; Gottardi and Teyssier, 2013), suggesting that there is no microstructural evidence for such temperature variations. Additionally, geochronological studies demonstrate that deformation and exhumation of the RRDSZ occurred contemporaneously and rapidly and was not temporally partitioned (~5 m.y.; Wells et al., 2000; Gottardi et al., 2015). Finally, there is no field evidence for structural telescoping; the RRDSZ does not exhibit any subsidiary detachment surfaces (e.g., Compton, 1980; Wells, 1997; Wells et al., 2000). Therefore, we assume that all studied samples experienced the same temperature conditions at the same time during exhumation, and that changes in RxGS are not related to temperature variations.

The observed RxGS differences could also be explained by differences in strain rate. The strain rate of the RRDSZ has previously been estimated to range between  $10^{-14}$  to  $10^{-13} \text{ s}^{-1}$  based on finite strain and thermochronological data (Wells et al., 2000; Gottardi and Teyssier, 2013). These rates are systematically at least one order of magnitude slower than strain rates determined from RxGS analysis, except those for the purest quartzite samples (Fig. 4). Besides demonstrating changes in muscovite content within the mylonites, the RRDSZ is devoid of any evidence of high-strain zones and rather accommodated strain homogeneously (e.g., Sullivan, 2008).

Variation in RxGS could be related to variations in stress at constant temperature. It is generally accepted that detachment shear zones evolve under constant stress (Behr and Platt, 2011). Subsidiary shear zones and rheological contrast between units may concentrate stress and deformation on various scales. However, as mentioned above, the RRDSZ lacks any subsidiary structures that may have localized stress locally and is localized entirely in the Elba Quartzite. The only lithological variation results from variation in muscovite content.

Because exhumation of the Raft River metamorphic core complex occurred rapidly and the RRDSZ is devoid of macro- and microstructural evidence of polyphase deformation or brittle overprint of the ductile microstructures, we thus (1) interpret the observed range of fabrics to reflect one event rather than the sum of several overprinting fabrics, and (2) attribute textural variation to phyllosilicate control over deformation and strain localization processes. This interpretation is consistent with experimental results (Tullis and Wenk, 1994; Tokle et al., 2023) and previous qualitative observations of texture variation in polyphase mylonites (e.g., Song and Ree, 2007; Herwigh et al., 2011; Hunter et al., 2016; Wehrens et al., 2017).

Paleopiezometric and strain rate calculations based on microstructural analysis are commonly applied to tectonic inferences of local and regional structures (e.g., Hirth et al., 2001; Gueydan et al., 2005; Behr and Platt, 2011; Gottardi and Teyssier, 2013; Lusk and Platt, 2020). Our results support the conclusions of laboratory studies (e.g., Tokle et al., 2023) that demonstrate that failure to account for phyllosilicate content may lead to erroneous results.

## CONCLUSION

In this project, we have investigated the effect of muscovite on quartz deformation in the RRDSZ. Our results demonstrate a strong inverse relationship between quartz RxGS and muscovite content both between samples and within sub-millimeter-scale subregions within individual samples. The range in grain sizes between our proximal samples translates into variation in calculated strain rate of greater

than one order of magnitude ( $\sim 1.1 \times 10^{-14}$  to  $2.4 \times 10^{-13}$  s $^{-1}$ ) and more than doubling of the calculated flow stress from most- to least-pure quartzite (32–70 MPa). These estimates are incompatible with previous field and thermochronology integrated strain rate estimates of the RRDSZ. Elsewhere, similar textural observations have been interpreted as evidence for polyphase deformation, reactivation, and superposition. We offer a simpler explanation that relatively small amounts of mica exert a disproportionate influence on quartz deformation fabrics, which has important implications for the application of flow laws in quartzite mylonites and the interpretation of strain localization mechanisms.

## ACKNOWLEDGMENTS

We thank the University of Texas High-Resolution X-ray Computed Tomography Facility for data acquisition and Hanna Romy for help with data processing. This research was funded through National Science Foundation grant EAR-Tectonics 1849812 (Gottardi and Casale). We thank editor Rob Strachan and reviewers John Platt, Andreas Kronenberg, Ryan Thigpen, and Rick Law for their reviews and constructive advice.

## REFERENCES CITED

Behr, W.M., and Platt, J.P., 2011, A naturally constrained stress profile through the middle crust in an extensional terrane: *Earth and Planetary Science Letters*, v. 303, p. 181–192, <https://doi.org/10.1016/j.epsl.2010.11.044>.

Compton, R.R., 1980, Fabrics and strains in quartzites of a metamorphic core complex, Raft River Mountains, Utah, in Crittenden, M.D., Jr., et al., eds., *Cordilleran Metamorphic Core Complexes: Geological Society of America Memoir 153*, p. 385–398, <https://doi.org/10.1130/MEM153-p385>.

Cross, A.J., Prior, D.J., Stipp, M., and Kidder, S., 2017, The recrystallized grain size piezometer for quartz: An EBSD-based calibration: *Geophysical Research Letters*, v. 44, p. 6667–6674, <https://doi.org/10.1002/2017GL073836>.

De Bresser, J.H.P., Peach, C.J., Reijns, J.P.J., and Spiers, C.J., 1998, On dynamic recrystallization during solid state flow: Effects of stress and temperature: *Geophysical Research Letters*, v. 25, p. 3457–3460, <https://doi.org/10.1029/98GL02690>.

De Bresser, J., Ter Heege, J., and Spiers, C., 2001, Grain size reduction by dynamic recrystallization: Can it result in major rheological weakening?: *International Journal of Earth Sciences*, v. 90, p. 28–45, <https://doi.org/10.1007/s005310000149>.

Etheridge, M.A., and Wilkie, J.C., 1979, Grain-size reduction, grain boundary sliding and the flow strength of mylonites: *Tectonophysics*, v. 58, p. 159–178, [https://doi.org/10.1016/0040-1951\(79\)90327-5](https://doi.org/10.1016/0040-1951(79)90327-5).

Fukuda, J.I., Holyoke, C.W., III, and Kronenberg, A.K., 2018, Deformation of fine-grained quartz aggregates by mixed diffusion and dislocation creep: *Journal of Geophysical Research: Solid Earth*, v. 123, p. 4676–4696, <https://doi.org/10.1029/2017JB015133>.

Gerbi, C., Culshaw, N., and Marsh, J., 2010, Magnitude of weakening during crustal-scale shear zone development: *Journal of Structural Geology*, v. 32, p. 107–117, <https://doi.org/10.1016/j.jsg.2009.10.002>.

Gottardi, R., and Teyssier, C., 2013, Thermomechanics of an extensional shear zone, Raft River metamorphic core complex, NW Utah: *Journal of Structural Geology*, v. 53, p. 54–69, <https://doi.org/10.1016/j.jsg.2013.05.012>.

Gottardi, R., Teyssier, C., Mulch, A., Vennemann, C.W., and Wells, M.L., 2011, Preservation of an extreme transient geotherm in the Raft River detachment shear zone: *Geology*, v. 39, p. 759–762, <https://doi.org/10.1130/G31834.1>.

Gottardi, R., Teyssier, C., Mulch, A., Valley, J.W., Spicuzza, M.J., Vennemann, T.W., Quilichini, A., and Heizler, M., 2015, Strain and permeability gradients traced by stable isotope exchange in the Raft River detachment shear zone, Utah: *Journal of Structural Geology*, v. 71, p. 41–57, <https://doi.org/10.1016/j.jsg.2014.10.005>.

Gueydan, F., Mehl, C., and Parra, T., 2005, Stress-strain rate history of a midcrustal shear zone and the onset of brittle deformation inferred from quartz recrystallized grain size, in Gapais, D., et al., eds., *Deformation Mechanisms, Rheology and Tectonics: From Minerals to the Lithosphere*: Geological Society, London, Special Publication 243, p. 127–142, <https://doi.org/10.1144/GSL.SP.2005.243.01.10>.

Herwegen, M., Linckens, J., Ebert, A., Berger, A., and Brodhag, S.H., 2011, The role of second phases for controlling microstructural evolution in polymimetic rocks: A review: *Journal of Structural Geology*, v. 33, p. 1728–1750, <https://doi.org/10.1016/j.jsg.2011.08.011>.

Hirth, G., and Tullis, J., 1992, Dislocation creep regimes in quartz aggregates: *Journal of Structural Geology*, v. 14, p. 145–159, [https://doi.org/10.1016/0191-8141\(92\)90053-Y](https://doi.org/10.1016/0191-8141(92)90053-Y).

Hirth, G., Teyssier, C., and Dunlap, J.W., 2001, An evaluation of quartzite flow laws based on comparisons between experimentally and naturally deformed rocks: *International Journal of Earth Sciences*, v. 90, p. 77–87, <https://doi.org/10.1007/s005310000152>.

Holyoke, C.W., III, and Tullis, J., 2006, Formation and maintenance of shear zones: *Geology*, v. 34, p. 105–108, <https://doi.org/10.1130/G22116.1>.

Hunter, N.J.R., Hasalová, P., Weinberg, R.F., and Wilson, C.J.L., 2016, Fabric controls on strain accommodation in naturally deformed mylonites: The influence of interconnected micaceous layers: *Journal of Structural Geology*, v. 83, p. 180–193, <https://doi.org/10.1016/j.jsg.2015.12.005>.

Johnson, S.E., Vernon, R.H., and Upton, P., 2004, Foliation development and progressive strain-rate partitioning in the crystallizing caprace of a tonalite pluton: Microstructural evidence and numerical modeling: *Journal of Structural Geology*, v. 26, p. 1845–1865, <https://doi.org/10.1016/j.jsg.2004.02.006>.

Kronenberg, A., 1981, Quartz preferred orientations within a deformed pebble conglomerate from New Hampshire, U.S.A.: *Tectonophysics*, v. 79, p. T7–T15, [https://doi.org/10.1016/0040-1951\(81\)90228-6](https://doi.org/10.1016/0040-1951(81)90228-6).

Law, R.D., Jessup, M.J., Searle, M.P., Francis, M.K., Waters, D.J., and Cottle, J.M., 2011, Telescoping of isotherms beneath the South Tibetan Detachment System, Mount Everest Massif: *Journal of Structural Geology*, v. 33, p. 1569–1594, <https://doi.org/10.1016/j.jsg.2011.09.004>.

Lusk, A.D., and Platt, J.P., 2020, The deep structure and rheology of a plate boundary-scale shear zone: Constraints from an exhumed Caledonian shear zone, NW Scotland: *Lithosphere*, v. 2020, no. 1, <https://doi.org/10.2113/2020/8824736>.

Mees, F., Swennen, R., Van Geet, M., and Jacobs, P., 2003, Applications of X-ray computed tomography in the geosciences, in Mees, F., et al., eds., *Applications of X-Ray Computed Tomography in the Geosciences*: Geological Society, London, Special Publication 215, p. 1–6, <https://doi.org/10.1144/GSL.SP.2003.215.01.01>.

Montési, L.G., 2013, Fabric development as the key for forming ductile shear zones and enabling plate tectonics: *Journal of Structural Geology*, v. 50, p. 254–266, <https://doi.org/10.1016/j.jsg.2012.12.011>; erratum available at <https://doi.org/10.1016/j.jsg.2014.07.001>.

Olgaard, D.L., 1990, The role of second phase in localizing deformation, in Knipe, R.J., and Rutter, E.H., eds., *Deformation Mechanisms, Rheology and Tectonics: Geological Society, London, Special Publication 54*, p. 175–181, <https://doi.org/10.1144/GSL.SP.1990.054.01.17>.

Prior, D.J., et al., 1999, The application of electron backscatter diffraction and orientation contrast imaging in the SEM to textural problems in rocks: *American Mineralogist*, v. 84, p. 1741–1759, <https://doi.org/10.2138/am-1999-11-1204>.

Rast, M., and Ruh, J.B., 2021, Numerical shear experiments of quartz-biotite aggregates: Insights on strain weakening and two-phase flow laws: *Journal of Structural Geology*, v. 149, <https://doi.org/10.1016/j.jsg.2021.104375>.

Richter, B., Stünitz, H., and Heilbronner, R., 2018, The brittle-to-viscous transition in polycrystalline quartz: An experimental study: *Journal of Structural Geology*, v. 114, p. 1–21, <https://doi.org/10.1016/j.jsg.2018.06.005>.

Song, W.J., and Ree, J.-H., 2007, Effect of mica on the grain size of dynamically recrystallized quartz in a quartz-muscovite mylonite: *Journal of Structural Geology*, v. 29, p. 1872–1881, <https://doi.org/10.1016/j.jsg.2007.09.011>.

Sullivan, W.A., 2008, Significance of transport-parallel strain variations in part of the Raft River shear zone, Raft River Mountains, Utah, USA: *Journal of Structural Geology*, v. 30, no. 2, p. 138–158, <https://doi.org/10.1016/j.jsg.2007.11.007>.

Taylor, S.R., and McLennan, S.M., 1985, *The Continental Crust: Its Composition and Evolution*: Oxford, UK, Blackwell Scientific, 312 p.

Tokle, L., Hirth, G., and Stünitz, H., 2023, The effect of muscovite on the microstructural evolution and rheology of quartzite in general shear: *Journal of Structural Geology*, v. 169, <https://doi.org/10.1016/j.jsg.2023.104835>.

Tullis, J., and Wenk, H.-R., 1994, Effect of muscovite on the strength and lattice preferred orientations of experimentally deformed quartz aggregates: *Materials Science and Engineering: A*, v. 175, p. 209–220, [https://doi.org/10.1016/0921-5093\(94\)91060-X](https://doi.org/10.1016/0921-5093(94)91060-X).

Tullis, J., and Yund, R.A., 1991, Diffusion creep in feldspar aggregates: Experimental evidence: *Journal of Structural Geology*, v. 13, p. 987–1000, [https://doi.org/10.1016/0191-8141\(91\)90051-J](https://doi.org/10.1016/0191-8141(91)90051-J).

Wehren, P., Baumberger, R., Berger, A., and Herwegen, M., 2017, How is strain localized in a meta-granitoid, mid-crustal basement section? Spatial distribution of deformation in the central Aar massif (Switzerland): *Journal of Structural Geology*, v. 94, p. 47–67, <https://doi.org/10.1016/j.jsg.2016.11.004>.

Wells, M.L., 1997, Alternating contraction and extension in the hinterlands of orogenic belts: An example from the Raft River Mountains, Utah: *Geological Society of America Bulletin*, v. 109, p. 107–126, [https://doi.org/10.1130/0016-7606\(1997\)109<0107:AEIT>2.3.CO;2](https://doi.org/10.1130/0016-7606(1997)109<0107:AEIT>2.3.CO;2).

Wells, M.L., Snee, L.W., and Blythe, A.E., 2000, Dating of major normal fault systems using thermochronology: An example from the Raft River detachment, Basin and Range, western United States: *Journal of Geophysical Research*, v. 105, p. 16,303–16,327, <https://doi.org/10.1029/2000JB900094>.

Printed in the USA